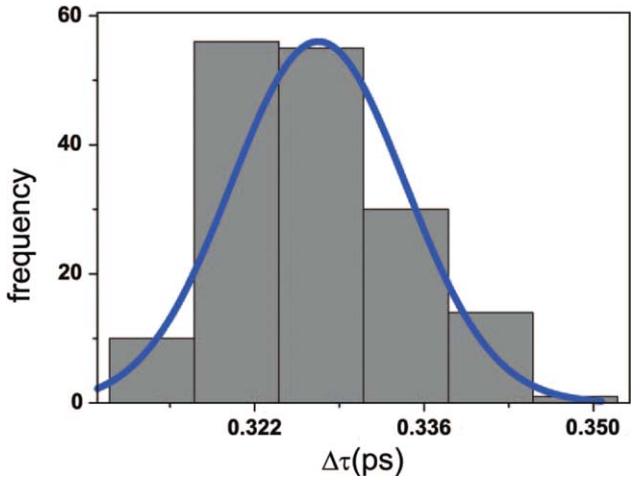

Figure 6 Histogram of all DGD values for Reel 2. [Color figure can be viewed in the online issue, which is available at www.interscience.wiley.com]

Two optical fiber reels with 50 km of the same manufacturer, factory rolled, were tested.

3. RESULTS AND DISCUSSION

After the implementation of the system, several acquisitions were taken in both reels. A typical interference pattern detected is shown in Figure 3. To convert this pattern to one similar to the one in Figure 1, it is necessary to find out the absolute value in relation to the mean intensity (see Fig. 4). Once that is done, the envelopes are adjusted to each pattern, thus making it possible to determine the instant DGD from the scanned distance, $2\Delta\tau = 2l/c$.

Comparing the interference patterns with the one in Figure 1, it can be assumed that we are in the presence of a noncoupled case because it clearly shows that the mode-coupling effect during the acquisitions did not reach levels high enough for this to be considered a high mode-coupling case. Then, nonmode-coupling approach is used.

As each interference pattern differs slightly from the previous one, to validate the statistical analysis [3], it was necessary to acquire several sets of patterns to calculate the PMD measurements.

For each reel, the acquisitions that were taken show a characteristic curve that closely resembles a Maxwell distribution of the expected time differential delay $<\Delta\tau>$, Figure 5. Using this value, it is possible to determine the PMD value using Eq. (2).

For Reel 1, the acquisitions were made over a time interval of 32 days. Whereas for Reel 2 (Figure 6), the acquisitions were made over a much smaller time frame—5 days—registering however, a greater number of measurements. In both cases, the PMD value was determined using Eq. (2) with the expected DGD value obtained from the interference patterns. The mean PMD value for Reel 1 was 0.0405 ± 0.0008 ps/km, while for Reel 2, the determined mean PMD value was 0.0463 ± 0.0004 ps/km. The existence of extreme PMD values very distant from the mean PMD value confirms that small variations of the initial parameters that affect birefringence cause unpredictable variations on the PMD value. The difference between PMD mean values for the two reels could be explained by the differences between their intrinsic properties in association with initial environmental conditions, temperature in particular, over a longer time frame for Reel 1 when compared with the 5-days time frame for Reel 2.

The PMD values can be determined straightforward using this setup and starting from the interference patterns. In the case of well-defined envelopes in the interference pattern (see Fig. 3), it is implied that the time delay between the two polarizations is greater than the coherence time of the source. When this condition is met, the DGD is easily determined from the interference pattern obtained with this setup. One limitation to PMD measurement can become visible when small and unpredictable variations of the states of polarization during the acquisition cause the fast and slow axis inside the reel to couple, thus altering the interference pattern profile.

4. CONCLUSIONS

The proposed low-coherence interferometry–based model proved to be a good method for PMD measurement, being only limited by the coherence time of the source to determinations of minimum DGD values of 0.13 ps. In this work, the minimum measured value was 0.14 ps.

As expected, probabilistic behavior of the first-order PMD was observed in the two 50-km optical fiber reels that were used. This reveals the influence that environmental factors have on PMD. One of these factors could be temperature and its variation can cause serious changes in the output states of polarization of the fiber.

REFERENCES

1. I.P. Kaminow and T.L. Koch, Optical fiber telecommunications iiia, Academic Press, London, 1997.
2. I.P. Kaminow, Polarization in optical fibers, IEEE J Quantum Electron 17 (1981), 15–22.
3. C.D. Poole, Statistical treatment of polarization dispersion in single-mode fiber, Opt Lett 13 (1988), 687–689.
4. P. Williams, PMD measurement techniques and how to avoid the pitfalls, Polarization Mode Dispersion 296 (2005), 133–154.
5. E. Simova, I. Powell, and C.P. Grover, Biased pi-shifted low-coherence interferometry for measuring polarization mode dispersion (pmd), Opt Fiber Technol 8 (2002), 4–23.
6. N. Cyr, Polarization-mode dispersion measurement: Generalization of the interferometric method to any coupling regime, J Lightwave Technol 22 (2004), 794–805.

WIRELESS PASSIVE PHOTO DETECTOR FOR INSECT TRACKING

Ville Viikari,[1] Jonathan Chisum,[2] and Heikki Seppä[1]
[1] VTT Technical Research Centre of Finland, Wireless Sensors, P.O.Box 1000, FI-02044 VTT, Finland; Corresponding author: ville.viikari@vtt.fi
[2] University of Colorado at Boulder, Boulder, Colorado 80305

Received 29 December 2009

ABSTRACT: *This letter presents a passive wireless photo detector for precise localization of insects in biological studies. The detector is based on a photo diode matched to an antenna, and it produces*

modulated backscattering of microwaves when illuminated with amplitude modulated light. The radar cross section of the detector is derived and the concept is experimentally verified at 1.5 GHz.
 Microwave Opt Technol Lett 52:2312–2315, 2010; Published online in Wiley InterScience (www.interscience.wiley.com). DOI 10.1002/mop.25427

Key words: *animals; photodiodes; tracking; transponders; wireless sensors*

1. INTRODUCTION

Several remote sensing and telemetric insect tracking techniques are developed for the demands of biological and agricultural studies. Remote sensing techniques do not require any physical interaction with the target whereas the insect is equipped with a transponder in telemetric techniques. A review of the techniques can be found in Ref. 1.

The remote sensing techniques used include, for example radar, video graphic and other optical techniques, X-ray imaging, and passive and active acoustical techniques. The advantage of remote sensing techniques is that they do not affect the insect behavior. However, as compared to telemetric techniques remote sensing techniques usually suffer from short detection distance and unreliable target identification.

Telemetric techniques include passive and active radio frequency identification (RFID), radio beacons [2], and harmonic radar. Active RFID and radio beacons are typically heavy and can be used only with large pedestrian insects. Passive RFID suffers from limited localization accuracy and short range. The harmonic radar transmits at one frequency and detects reflections at harmonic frequencies, which are generated by a passive harmonic transponder attached to the tracked insect. An advantage of the harmonic radar over conventional radar is its ability to track small radar targets that are close to cluttering objects, such as ground or vegetation.

The harmonic radar concept was first proposed for traffic applications [3] and later was used for locating avalanche victims [4] and tracking insects such as bees [5–7], butterflies [8, 9], and moths [10]. Harmonic radar concepts for insect tracking are discussed in Refs. 6, 8, and 11.

The drawbacks of the harmonic radar is that it is difficult to comply with frequency regulations due to the large harmonic frequency offset, it has limited angular resolution due to antenna beam width, it typically uses very high transmit power (25 kW peak power) [6], and it requires mechanical scanning. Traditional harmonic radar does not lend itself well to indoor use.

This article presents a telemetric insect tracking technique that provides precise (millimeters accuracy) insect localization in indoor arenas and cages, can be implemented with a relatively simple system, and that provides lightweight transponders. The technique utilizes a passive wireless photo detector as a photo-activated microwave transponder. The detector consists of a photo diode matched to an antenna, and it produces modulated backscatter at microwave frequencies when illuminated with amplitude modulated light, for example, a laser beam. The detector enables lightweight implementation and offers the possibility to use fast laser scanners for precise target localization. In addition to insect tracking, the wireless photo detector can be utilized in various applications, where a lightweight transponder needs to be precisely located or a wireless photo detector is needed.

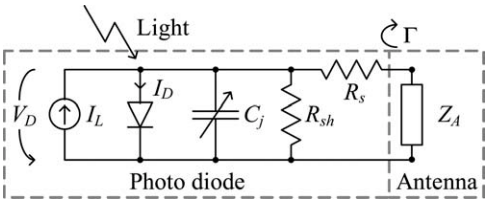

Figure 1 An electrical equivalent circuit of the wireless photo detector

2. PHOTO-ACTIVATED TRANSPONDER

The wireless photo detector consists of a photo diode that is matched to an antenna. The equivalent electrical circuit of the detector is shown in Figure 1.

The absorbed photons create electron-hole-pairs in the diode. The procedure is described with a current generator, whose current as a function of the absorbed light power P_L is given as $I_L = P_L R_\lambda$, where R_λ is the responsivity (typically ~0.5 A/W) of the diode. The diode current is given as

$$I_D = I_{sat}\left(e^{-\frac{qV_D}{\eta kT}} - 1\right), \tag{1}$$

where η is the ideality factor, $k = 1.38 \times 10^{-23}$ J/K is Boltzmann's constant, T is the temperature, $q = 1.60 \times 10^{-19}$C is the elementary charge, I_{sat} is the saturation current, and V_D is the voltage across the diode. Let us assume that the shunt resistance and antenna impedance, R_{sh} and Z_A (in Fig. 1) are very large (at low optical modulation frequency). Then, the voltage across the diode can be written as

$$V_D = \frac{\eta kT}{q}\ln\left(\frac{P_L R_\lambda + I_{sat}}{I_{sat}}\right). \tag{2}$$

The voltage affects both the junction resistance and capacitance. The small-signal junction resistance of the diode is

$$r_j = \frac{1}{dV/dI} = \frac{\eta kT}{qI_{sat}} e^{-\frac{qV_D}{\eta kT}}. \tag{3}$$

The junction capacitance is given as

$$C_j = C_{j0}\left(1 - \frac{V_D}{\Phi_i}\right)^{-\gamma}, \tag{4}$$

where Φ_i is the junction potential and γ is the profile parameter for the depletion capacitance and is 0.5 for a uniformly doped junction.

The diode is illuminated with a light source whose amplitude is square-wave modulated. The light absorbed by the diode is given as

$$P_L(t)\begin{cases} P_{L1}, & \frac{k-1/2}{f_m} < t < \frac{k}{f_m} \\ P_{L2}, & \frac{k}{f_m} < t < \frac{k+1/2}{f_m} \end{cases}, \tag{5}$$

TABLE 1 The Parameters of the Photo Diode

Sensitivity	$R_\lambda = 0.55$ A/W
Junction capacitance at zero bias[a]	$C_{j0} = 0.94$ pF
Series resistance	$R_s = 12\Omega$
Saturation current[a]	$I_{sat,d} = 8.7\ \mu$A
Junction potential	$\Phi_i = 1$V
Shunt resistance	$R_{sh} = 10$ MΩ
Radiant sensitive area (chip)	$A = 0.78$ mm^2
Radiant sensitive area (packed diode)	$A = 20$ mm^2
Series inductance due to package[a]	$L_s = 3.5$ nH

[a] Fitted to the measurements.

where f_m is the modulation frequency and k is an integer. The modulated illumination changes the diode impedance between two states, $Z_{d,1}$ and $Z_{d,2}$, and causes modulated backscatter. The modulated radar cross section (RCS) of the transponder is given as [12]

$$\sigma_m = \frac{G^2\lambda^2}{2\pi^3}|\Gamma_1 - \Gamma_2|^2, \tag{6}$$

where G is the antenna gain, λ is the wavelength, and Γ_i is the reflection coefficient given as

$$\Gamma_i = \frac{Z_{d,i} - Z_A^*}{Z_{d,i} + Z_A}, \tag{7}$$

where * denotes complex conjugate.

3. EXPERIMENTS

3.1. Irradiance Response of the Diode Impedance

A BPV10 photo diode (Vishay Semiconductors) is used in the experimental wireless photo detector. The diode parameters are shown in Table 1.

The impedance of the diode at different irradiance levels is measured with a network analyzer (4294A, Agilent Technologies). The photo diode is illuminated with a power LED, and the irradiance level at the diode is measured with a spectrometer (HR4000, Ocean Optics). The ambient light is blocked by placing the LED and the diode inside a black box.

The measured real and imaginary parts of the diode impedance at different irradiance levels at 1.5 GHz are shown in Figure 2 with the calculated curves. The diode ideality factor is assumed to be $\eta = 1$ and the junction profile parameter $\gamma = 0.5$ in the calculation.

The calculated and measured impedances agree well and show that the simple model of the photo diode in Figure 1 can be used for designing a wireless photo detector. Figure 2 also shows that very strong modulation is achieved at relatively low irradiance levels. Therefore, even a low power class I-laser scanner, whose laser power is limited to 1 mW, could be used for locating the target.

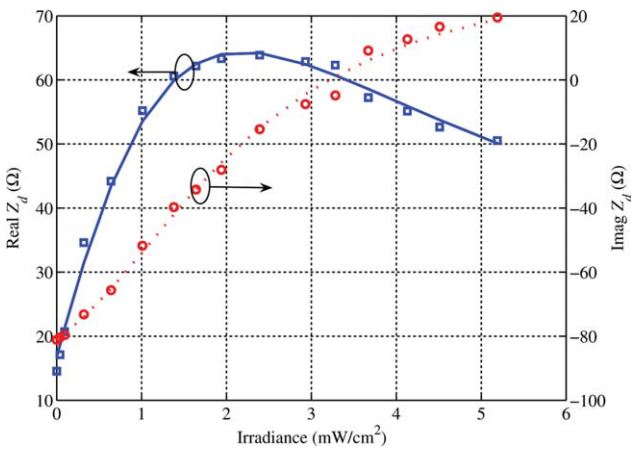

Figure 2 The measured (marker) and calculated (line) impedance of the photo diode at 1.5 GHz as a function of irradiance. [Color figure can be viewed in the online issue, which is available at www.interscience.wiley.com]

3.2. Wireless Photo Detector

The wireless photo detector is implemented by attaching an antenna to the diode. The transponder performance is heavily determined by the antenna and the antenna impedance should be optimized for the diode impedance at the expected irradiance levels. For example, the measured diode impedances at 0 and 1 mW/cm^2 irradiance levels at 1.5 GHz are $Z_{d,1} = (14.5 - j81)\Omega$ and $Z_{d,2} = (34.6 - j73)\Omega$, respectively. The antenna impedance that provides the largest modulated RCS is solved from

$$\max_{Z_A}\left\{\left|\frac{Z_{d,1} - Z_A^*}{Z_{d,1} + Z_A} - \frac{Z_{d,2} - Z_A^*}{Z_{d,2} + Z_A}\right|^2\right\}. \tag{8}$$

Numerical solution of Eq. (8) gives the optimal antenna impedance of $Z_A = (22 + j78)\Omega$. The modulated power reflection coefficient for that impedance is $|\Gamma_1 - \Gamma_2|^2 = 0.2$.

A small loop antenna is used in the transponder. The loop is formed of 0.3 mm thick copper wire and its radius is 7 mm. Theoretical calculations give a loop impedance of $(0.9 + j325)\Omega$ at 1.5 GHz. This could be transformed to the optimal impedance adding a series capacitor of 0.31 pF and a shunt inductor of 1.45 nH to the antenna. The used component values were 0.56 pF and 1.5 nH. In addition to the matching elements, a 47 pF series capacitor was used between the diode and the antenna for DC-blocking. The diode was shunted with a 10 MΩ resistor to ensure low fall time and thus fast optical response.

A photograph of the transponder is shown in Figure 3. A packaged photo diode is used in this experiment due to poor availability of bare diode chips. A bare photo diode chip with an antenna optimized for low mass would enable a lightweight and small transponder. For example, a 1 mm × 1 mm × 0.2 mm size silicon diode chip weighs ~0.5 mg. Similarly, the loop antenna could be manufactured of 0.1 mm thick copper wire

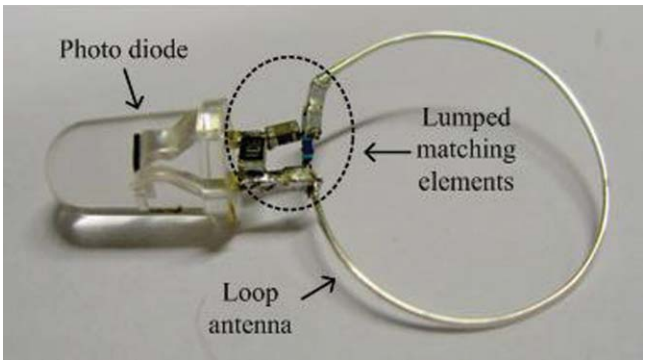

Figure 3 A photograph of the photo-activated microwave transponder. [Color figure can be viewed in the online issue, which is available at www.interscience.wiley.com]

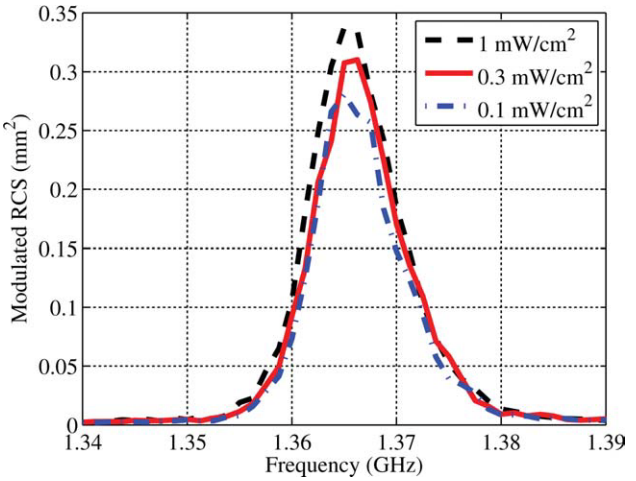

Figure 4 The measured modulated radar cross section (RCS) of the transponder. The curves are for different irradiance levels. [Color figure can be viewed in the online issue, which is available at www.interscience.wiley.com]

and matched directly to the diode without lumped elements. Such antenna with equal loop size to that used in the measurements would weigh 3 mg providing a transponder weight comparable to that of typical harmonic radar transponders (3 mg) [6]. Further size and mass reductions of the transponder could be achieved by using higher microwave frequencies for interrogation. This, however, could necessitate a smaller effective photo diode area and thus stronger laser illumination.

3.3. Modulated Radar Cross Section

The modulated RCS of the transponder is measured by illuminating it with a broad band horn antenna (EMCO 3115, Electro-Mechanics Co.) fed with a signal generator (Agilent E8257D). The backscattered signal at the optical offset frequency of the transmission is recorded with a horn antenna (BBHA 9120 A, Schwarzbeck) connected to a spectrum analyzer (Rohde & Schwarz FSEM). The transponder is illuminated with the square-wave modulated LED at 10 kHz. The measured modulated RCS of the transponder is shown in Figure 4.

The highest modulated RCS of the transponder occurs at 1.365 GHz and it is $\sim$0.3 mm^2 depending on the irradiance level. The measured modulated RCS is well in line with a theoretical estimate. For example, assuming ideal antenna matching and 0 dBi antenna directivity, 4.4% radiation efficiency, which is typical for electrically small loop antennas, would result into a 0.3 mm^2 modulated RCS at 1.36 GHz according to Eq. (6).

The prototype transponder could provide a reasonable microwave detection range. For example, assuming that the transponder is interrogated with a reader with 20 dBm transmit power, $-$110 dBm sensitivity, and 6 dBi antenna gain the transponder could be detected from 5.8 m microwave distance. This range would cover even relatively large insect cages with a small number of microwave antennas. If needed, the detection distance could be increased by using a better matched and more efficient transponder antenna.

Figure 4 shows that sufficient modulation occurs at irradiance levels as low as 0.1 mW/cm^2. If using a bare diode chip instead of a packaged photo diode, the irradiance level should be 20 times higher and a class I-laser (1 mW power) could be used to produce spots up to 7 $\times$ 7 mm in size. Further, assuming that a laser scanner with a 1 kHz scanning rate (which is typical for commercially available scanners) was used with 7 $\times$ 7 mm spot, 0.5 m^2 area could be scanned in a second.

4. CONCLUSIONS

We have presented a technique that is suitable for precise localization of insects in indoor arenas. The technique utilizes a wireless photo detector as a photo-activated microwave transponder. The transponder consists of an antenna matched to a photo diode and it produces modulated backscatter at microwave frequencies when illuminated by a modulated light source such as a laser. Our experimental demonstration at 1.36 GHz proved the concept, and we have shown that a lightweight (3 mg) transponder could be implemented at that frequency and that its detection distance could be $\sim$6 m, which enables to cover even large insect cages with relatively low number of antennas. We have also shown that sufficient modulation of the transponder occurs at irradiance levels as low as 2 mW/cm^2. A typical class I laser scanner could provide 7 mm position accuracy and could scan areas up to 0.5 m^2/s.

ACKNOWLEDGMENT

This research was supported in part by the Academy of Finland under decision 132982 and by the EU Commission under FP7-ICT-2007-1-216049 of the ADOSE project.

REFERENCES

1. D.R. Reynolds and J.R. Riley, Remote-sensing, telemetric and computer-based technologies for investigating insect movement: A survey of existing and potential techniques, Comput Electron Agri 35 (2002), 271–307.
2. J. Hedin and T. Ranius, Using radio telemetry to study dispersal of the beetle *Osmoderma eremita*, Comput Electron Agri 35 (2002), 171–180.
3. H. Staras and J. Shefer, Harmonic radar detecting and ranging system for automotive vehicles, US Patent 3,781,879 (1972).
4. Available at: http://recco.com/.
5. E.A. Capaldi, A.D. Smith, J.L. Osborne, S.E. Fahrbach, S.M. Farris, D.R. Reynolds, A.S. Edwards, A. Martin, G.E. Robinson, G.M. Poppy, and J.R. Riley, Ontogeny of orientation flight in the honeybee revealed by harmonic radar, Nature 403 (2002), 537–540.
6. J.R. Riley and A.D. Smith, Design considerations for an harmonic radar to investigate the flight of insects at low altitude, Comput Electron Agri 35 (2002), 151–169.
7. J.L. Osborne, S.J. Clark, R.J. Morris, I.H. Williams, J.R. Riley, A.D. Smith, D.R. Reynolds, and A.S. Edwards, A landscape-scale study of bumblebee foraging range and constancy, using harmonic radar, J Appl Ecol 36 (1999), 519–533.
8. E.T. Cant, A.D. Smith, D.R. Reynold, and J.L. Osborne, Tracing butterfly flight paths across the landscape with harmonic radar, Proc R Soc B Biol Sci 272 (2005), 785–790.
9. O. Ovaskainen, A.D. Smith, J.L. Osborne, D.R. Reynolds, N.L. Carreck, A.P. Martin, K. Niitepold, and I. Hanski, Tracking butterfly movements with harmonic radar reveals an effect of population age on movement distance, Proc Natl Acad Sci 105 (2008), 19090–19095.
10. G.P. Svensson, P.G. Valeur, D.R. Reynolds, A.D. Smith, J.R. Riley, T.C. Baker, G.M. Poppy, and C. Löfstedt, Mating disruption in *Agrotis segetum* monitored by harmonic radar, Entomologia Experimentalis et Applicata 101 (2001), 111–121.
11. B.G. Colpitts and G. Boiteau, Harmonic radar transceiver design: Miniature tags for insect tracking, IEEE Trans Antennas Propag 52 (2004), 2825–2832.
12. P. Pursula, Analysis and design of UHF and millimetre wave radio frequency identification, D.Sc. Dissertation, Faculty of Information and Natural Sciences, Helsinki University of Technology, Espoo, Finland, 2008.